11664 *Biochemistry* **2009,** *48,* 11664–11677
DOI: 10.1021/bi901351q

BIOCHEMISTRY
including biophysical chemistry & molecular biology
Article

Distinct Pose of Discodermolide in Taxol Binding Pocket Drives a Complementary Mode of Microtubule Stabilization†

Marina Khrapunovich-Baine,‡ Vilas Menon,§ Pascal Verdier-Pinard,∥ Amos B. Smith III,⊥ Ruth Hogue Angeletti,# Andras Fiser,§ Susan Band Horwitz,*,‡,△ and Hui Xiao#,△

‡*Department of Molecular Pharmacology,* §*Department of Systems and Computational Biology,* #*Laboratory of Macromolecular Analysis and Proteomics, Albert Einstein College of Medicine, Bronx, New York 10461,* ∥*INSERM UMR 911 CR02, Aix-Marseille Université, 132855 Marseille Cedex 05, France, and* ⊥*Department of Chemistry, University of Pennsylvania, Philadelphia, Pennsylvania 19104* △*Co-senior authors*

Received August 4, 2009; Revised Manuscript Received October 26, 2009

ABSTRACT: The microtubule cytoskeleton has proven to be an effective target for cancer therapeutics. One class of drugs, known as microtubule stabilizing agents (MSAs), binds to microtubule polymers and stabilizes them against depolymerization. The prototype of this group of drugs, Taxol, is an effective chemotherapeutic agent used extensively in the treatment of human ovarian, breast, and lung carcinomas. Although electron crystallography and photoaffinity labeling experiments determined that the binding site for Taxol is in a hydrophobic pocket in β-tubulin, little was known about the effects of this drug on the conformation of the entire microtubule. A recent study from our laboratory utilizing hydrogen−deuterium exchange (HDX) in concert with various mass spectrometry (MS) techniques has provided new information on the structure of microtubules upon Taxol binding. In the current study we apply this technique to determine the binding mode and the conformational effects on chicken erythrocyte tubulin (CET) of another MSA, discodermolide, whose synthetic analogues may have potential use in the clinic. We confirmed that, like Taxol, discodermolide binds to the taxane binding pocket in β-tubulin. However, as opposed to Taxol, which has major interactions with the M-loop, discodermolide orients itself away from this loop and toward the N-terminal H1−S2 loop. Additionally, discodermolide stabilizes microtubules mainly via its effects on interdimer contacts, specifically on the α-tubulin side, and to a lesser extent on interprotofilament contacts between adjacent β-tubulin subunits. Also, our results indicate complementary stabilizing effects of Taxol and discodermolide on the microtubules, which may explain the synergy observed between the two drugs *in vivo*.

Microtubule-stabilizing agents (MSAs)[1] comprise a class of drugs that bind to polymerized microtubules (MTs) and inhibit their disassembly into the dimeric $\alpha\beta$-tubulin components. Thus, the primary cellular response to these drugs is arrest in mitosis due to inhibition of microtubule dynamics in the mitotic spindle. Taxol is the prototype of the MSAs, used extensively in the clinic to treat ovarian, breast, and lung carcinomas (*1*). The drug binds to the β-tubulin subunit of the microtubule (*2*) and promotes polymerization in the absence of GTP, which is normally required for polymer formation (*3*). Studies with photoaffinity-labeled Taxol analogues conducted in our laboratory (*4*−*6*) and the development of a high-resolution structure of the $\alpha\beta$-tubulin dimer (*7*, *8*) identified the Taxol binding site in β-tubulin. Later, several Taxol binding conformations in the lumen of β-tubulin in the microtubules have been proposed (*9*−*11*). Recently, our laboratory utilized, for the first time, hydrogen−deuterium exchange (HDX) coupled to liquid chromatography−electrospray ionization mass spectrometry (LC-ESI MS) to determine specific conformational effects of Taxol on microtubules (*12*), which provided insights into the mechanisms of MT stabilization by this drug and gave us new and accurate means to study the effects of MSAs on MT conformation.

Although Taxol is an effective chemotherapeutic agent, it has low aqueous solubility and a propensity for the development of resistance in patients (*13*). This has led to a search for new MSAs with enhanced therapeutic activity. One of the drugs identified in this search was discodermolide, which is a weaker substrate for P-glycoprotein than Taxol and has an aqueous solubility estimated at 160-fold greater than that of Taxol (*14*).

Discodermolide, isolated from a marine sponge, *Discodermia dissoluta* (*14*), was originally reported to be a potential immunosuppressive agent (*15*, *16*), but was later found to interact with microtubules in a manner similar to that of Taxol (*17*). Further studies, however, revealed clear differences between the two drugs. *In vitro*, discodermolide exhibits a greater polymerization potency than Taxol on tubulin isolated from calf brain. Additionally, MTs formed in the presence of discodermolide are much shorter in length than those formed in the presence of Taxol (*14*). In competition assays with [^{3}H]Taxol (*17*), discodermolide demonstrates stronger affinity for bovine brain MTs. However, there is no cross-resistance to discodermolide in cell lines that are

†M.K.-B. is supported by a Pre-Doctoral Fellowship in Pharmacology/Toxicology from the PhRMA Foundation. This work was supported by National Cancer Institute Grant CA124898 and the National Foundation for Cancer Research (to S.B.H.).

*Corresponding author. Phone: (718) 430-2163. Fax: (718) 430-8959. E-mail: susan.horwitz@einstein.yu.edu.

[1]Abbreviations: MSA, microtubule stabilizing agent; MT, microtubule; CET, chicken erythrocyte tubulin; GTP, guanosine triphosphate; GDP, guanosine diphosphate; GMPCPP, guanosine-5′-[(α,β)-methylene]triphosphate; HDX, hydrogen−deuterium exchange; MS, mass spectrometry; LC-ESI, liquid chromatography electrospray ionization; FT-ICR MS, Fourier transform ion cyclotron resonance mass spectrometer; Disco, discodermolide.

 Published on Web 10/29/2009

resistant to Taxol due to mutations in β-tubulin; in particular, discodermolide does not substitute for Taxol in sustaining the growth of Taxol-dependent cell lines.(*17*, *18*) Interestingly, discodermolide can induce accelerated cell senescence, which is not a typical characteristic of Taxol (*19*).

Of particular relevance are the findings from our laboratory that discodermolide and Taxol act synergistically, both in cell culture and in an ovarian xenograft tumor model in nude mice (*20*, *21*). Additionally, in human nonsmall cell lung carcinoma cells, the combination of the two drugs has been shown to synergistically suppress microtubule dynamic instability (*22*). The distinct effects on MTs and the synergy observed between discodermolide and Taxol are most likely due to the subtle differences in their binding and induced conformational changes on MTs. To explore this hypothesis, our laboratory conducted a number of modeling and photoaffinity-labeled discodermolide analogue studies to determine the binding conformation of discodermolide (*23*, *24*). These experiments confirmed that the binding site for discodermolide is in the same drug-binding pocket of β-tubulin as Taxol and predicted the orientation of the discodermolide molecule at this site. NMR experiments later carried out by the Jiménez-Barbero group were only partially in agreement with these studies, such that the binding pocket was the same, but the orientation and some of the contacts made by discodermolide within it were different (*25*). Thus, the precise binding conformation for discodermolide is yet to be determined. Moreover, the conformational effects of discodermolide on microtubules remain elusive.

In our present study, we utilized HDX coupled to LC-ESI MS to redefine the binding site of discodermolide and to measure its effects on the conformation of the entire microtubule. Our results suggest that in tubulin isolated from chicken erythrocytes (CET) discodermolide binds, with a weaker affinity, to the luminal taxane binding site in β-tubulin with an orientation distinct from that shown in previous studies (*24*, *25*). Most of the conformational effects on MTs observed with Taxol are also seen with discodermolide, but to a lesser extent, which is consistent with our *in vitro* polymerization assays. The major differences between the two drugs, however, are observed in regions involved in lateral and longitudinal interactions between protofilaments and αβ-tubulin dimers, respectively. This implies a distinct mechanism for MT stabilization induced by discodermolide as compared to Taxol. In addition, our results suggest complementary stabilization by Taxol and discodermolide, which is a possible molecular basis for synergy between the two MSAs.

MATERIALS AND METHODS

Tubulin and Reagents. Tubulin was isolated from the marginal bands of chicken erythrocytes and from bovine brain as previously described (*24*, *26*). Bovine brain tubulin (BBT) was stored in 0.1 M MES, 1 mM EGTA, 0.5 mM $MgCl_2$, and 3 M glycerol, pH 6.6, in liquid nitrogen. Chicken erythrocyte tubulin (CET) used for GTP-free assembly was stored under the same conditions as BBT. CET used for assembly assays in the presence of GTP was stored in a 0.1 mM GTP buffer free of glycerol (0.1 M MES, 1 mM $MgCl_2$, 1 mM EGTA, 1 mM DTT, and 0.1 mM GTP, pH 6.8) and in liquid nitrogen. CET used for the mass spectrometry experiments was further purified on a phosphocellulose column (*26*) and stored as a 40 μM stock solution in a nucleotide-free buffer (50 mM MES, 1 mM EGTA, and 0.2 mM $MgCl_2$, pH 6.8) in liquid nitrogen. This tubulin contains a single α- and β-isotype, α1 and βVI, whose amino acid sequences are 95% and 83% identical to the corresponding human isotypes, respectively. Purity was 99%, as evaluated by SDS−PAGE and Coomassie staining, and isotype content was confirmed by high-resolution isoelectric focusing (not shown). Purified tubulin was fully functional as assessed by measuring its ability to polymerize at 37 °C in the presence of equimolar Taxol, and its morphology was normal, as determined by negative-staining transmission electron microscopy following assembly (not shown).

Taxol and [^{3}H]Taxol were obtained from the Drug Development Branch, National Cancer Institute, Bethesda, MD. Discodermolide was synthesized as previously described (*27*). Porcine stomach pepsin was purchased from Sigma-Aldrich. Deuterium oxide (99.9%) was obtained from Cambridge Isotope Laboratories. Tris(2-carboxyethyl)phosphine (TCEP, 0.5 M), guanidinium hydrochloride, formic acid (FA), and trifluoroacetic acid (TFA) were from Pierce. GMPCPP (100 mM) was purchased from Jena Bioscience, Germany. Acetonitrile was purchased from Fisher Scientific. All other reagents were of the highest purity available.

In Vitro Microtubule Polymerization Assays. Drugs were dissolved in DMSO (5 mM). Assays were done in a 300 μL quartz cuvette. CET, containing GTP, was diluted to 0.8 mg/mL in tubulin polymerization buffer (0.1 M MES, 1 mM EGTA, 0.5 mM $MgCl_2$, and 3 M glycerol, pH 6.7). GTP-free CET and BBT were diluted to 1.0 mg/mL. Assembly of microtubule protein was monitored spectrophotometrically (Beckman Coulter DU640) by recording changes in turbidity at 350 nm and 37 °C. For GTP-containing CET, after equilibration (*A* at 350 nm reached a plateau) 8 μM drug, 8 μM GTP, or an equal volume of DMSO (control) was added, and polymerization was further monitored. For GTP-free CET and BBT assembly, 10 μM drug or an equal volume of DMSO (control) was added.

Drug Displacement Studies. Three separate experiments were done as described previously (*24*, *28*, *29*). Briefly, 200 μL of 2 μM CET or 2 μM BBT was polymerized in the presence of 0.2 mM GTP and unlabeled Taxol or discodermolide. After incubation for 20 min at 37 °C, 2 μM [^{3}H]Taxol was added for another 2 h, and the samples were layered onto 20 μL of 5% sucrose in 0.1 M MES tubulin assembly buffer containing 3 M glycerol and centrifuged in a Ti42.2 rotor in a Beckman L7 ultracentrifuge at 100000*g* for 1 h at 27 °C. After centrifugation, the supernatant was carefully removed, and the pellet was washed three times with 0.1 M MES buffer and dissolved in 10 mM sodium phosphate buffer containing 1% SDS. Radioactivity was determined in a liquid scintillation counter (Perkin-Elmer). Relative amounts of [^{3}H]Taxol bound were measured as the ratio of counts per minute for $[\text{drug}]_{\text{unlabeled}}$ to $[\text{no drug}]_{\text{unlabeled}}$.

HDX/MS Experiments. For GMPCPP-induced assembly, tubulin was incubated at 40 μM (~7 times the critical concentration for assembly) in MEM buffer (50 mM MES, 1 mM EGTA, and 0.2 mM $MgCl_2$, pH 6.8) at 37 °C in the presence of 1 mM GMPCPP and DMSO (volume equal to the total drug volume used in the ligand samples) for 30 min. For drug experiments, tubulin was preincubated at 37 °C with 1 mM GMPCPP for 30 min. To ensure solubility, Taxol and discodermolide were added in three increments of increasing concentrations (10 μM, 100 μM, and 1 mM), and allowed to incubate for 10 min after the first two additions and 15 min after the last one. For global analysis, HDX on tubulin was initiated by diluting each sample 20-fold in 0.1 M deuterated MEM buffer, pD 6.9 at 37 °C.

Exchange was allowed to proceed for 1, 5, 10, 30, and 60 min, after which point the aliquot exchange solutions were quenched with equal volumes of ice-cold 0.5 M ammonium phosphate buffer (pH 2.5). The quenched samples were subjected to immediate LC-ESI MS analysis. As most labeling was complete after 20 min, a 30 min time point was selected for local HDX experiments. These were carried out similarly to the global experiments, with a few modifications to optimize sequence coverage. Namely, the initial tubulin dilution in the HDX buffer was reduced to only 3.5-fold to yield a final 10-fold dilution after quenching with denaturing buffer (0.5 M ammonium phosphate, 100% (w/v) guanidinium hydrochloride, and 2.5 mM TCEP, pH 2.5) and subjecting the samples to a digest with equimolar pepsin in solution (pH 2.1).

HDX LC-MS System and Peptide Identification. A Shimadzu HPLC, with two LC-10AD pumps, was used to generate a fast gradient with 30 μL/min flow rate, optimized for best sequence coverage. Solvent A was 5% acetonitrile in H_2O, 0.2% FA, and 0.01% TFA, while solvent B consisted of 95% acetonitrile in H_2O, 0.2% FA, and 0.01% TFA. All components of the setup, including tubing, injector, and column, were submerged in an ice bath at all times in order to reduce back-exchange. For global exchange experiments, 7 μL of quenched reaction mixture was injected onto a 1.0 mm i.d. $\times$ 50 mm C3 column (Micro-Tech Scientific Inc.). After desalting with 5% solvent B for 5 min, intact tubulin was eluted with a 2 min gradient composed of 5−95% B. The effluent was directly delivered to the LTQ mass spectrometer (Thermo Electron Corp.) for mass analysis. For analysis of proteolytic peptides, 20 μL of chilled digest was injected onto a 1.0 mm i.d. $\times$ 50 mm C8 column (Waters Inc.). After desalting for 5 min with 5% B, the peptides were eluted at 30 μL/min with a 5−10% gradient for 0.01 min, 10−40% for 10 min, 40−50% for 1 min, and 50−95% for 1 min. The effluent was infused into a 12 T Varian IonSpec FT-ICR MS (Varian Inc.). For peptide identification 30 s fractions were collected into a 96-well plate by coupling the HPLC with TriVersa NanoMate (Advion Inc.). Each fraction was spiked with an internal standard, and the mass spectra were collected by coupling chip-based infusion of the TriVersa NanoMate with the FT-ICR MS. The peptides were identified by a combination of accurate masses and MS/MS. The extent of deuterium incorporation of each peptic peptide was determined by FT-ICR MS from the centroid mass difference between deuterated and nondeuterated samples.

Data Analysis and Presentation. Average changes in deuterium incorporation (ΔHDX) $\pm$ standard deviations were determined from three separate experiments. Significance was determined based on a two-tailed *t*-test using standard deviations obtained from a single set of triplicate analyses of drug-saturated and drug-free microtubules on a per-peptide basis. Based on a combination of instrument accuracy and precision of data analysis the significance was set at $P < 0.05$. Thus any change in deuterium incorporation with $P < 0.05$ was considered significant even if the absolute average value for ΔHDX was below 0.5. Peptides that exhibited significant changes in deuterium incorporation were mapped onto the tubulin dimer structure (1JFF) and onto a structure of a microtubule protofilament pair previously constructed in our laboratory (*12*). Molecular representations of tubulin in all figures were generated using Pymol.[2]

Docking Simulations and Contact Map Generation. Flexible-ligand docking simulations were conducted with the program SURFLEX (*30*), using a previously developed protein structure model of chicken erythrocyte tubulin dimer (*12*). The initial chemical structures of taxol and discodermolide used to seed the docking simulations were generated using the DS Visualizer 2.0 software package.[3] The 20 top-scoring results from the docking runs were filtered to exclude configurations making excessive primary contacts with residues that were not protected by ligand binding, as determined by HDX data. In addition, a second docking run was conducted for discodermolide, using an observed NMR structure (*25*) of discodermolide as the initial structure and filtering the final results based on HDX data and on similarity to the original NMR-derived structure. In all cases, primary contacts were defined as those making direct contact with the ligand in the final docked configuration, as calculated using LPC software (*31*). Secondary contacts were defined as those making contact with the primary residues and not with the ligand itself, as calculated using CSU software (*31*). The overall contact maps were visualized using Visone software.[4]

RESULTS

CET Assembly and Drug Displacement Assays. Chicken erythrocyte tubulin, unlike tubulin isolated from other tissues, is composed of one α- and one β-tubulin isotype, α1 and βVI, respectively. In addition, it has very limited posttranslational modifications (*32*). When the highly divergent C-terminal residues are not considered, chicken βVI is 90% identical to human βI, the major isotype in nonneuronal tissue (Supporting Information Figure S1). These characteristics of chicken erythrocyte tubulin make it ideal to study using mass spectrometry, as it eliminates any ambiguity in the assignment of measured masses and potential conformational differences between different tubulin isotypes. Since we use chicken erythrocyte tubulin in the conformational studies, the binding of Taxol and discodermolide and their effects on microtubule assembly in this system were examined (Figure 1). In the presence of GTP, which best mimics the conditions of the HDX studies described below, Taxol and discodermolide exhibit similar effects on microtubule polymerization, as the overall change in turbidity after drug addition is the same for both drugs (Figure 1a). Neither DMSO (control) nor additional GTP had significant effects on polymerization (Figure 1a). The initiation of MT assembly is faster in the presence of Taxol than discodermolide, since the first time point after drug addition has a higher absorbance value at 350 nm when Taxol is used ($A_{Disco} = 0.011$, $A_{Taxol} = 0.054$). Moreover, displacement analysis of [^{3}H]Taxol with nonradiolabeled Taxol and discodermolide suggests that, unlike with calf brain tubulin (*17*, *33*), discodermolide is completely displaced by [^{3}H] Taxol from microtubules obtained from chicken erythrocytes (Figure 1b). This is consistent with the results of the GTP-free assembly assays, which showed that Taxol is a much stronger promoter of CET polymerization than discodermolide but a weaker promoter of BBT assembly (Supporting Information Figure S2).

Global HDX. We compared the time courses of HDX in chicken erythrocyte tubulin complexes with Taxol and with discodermolide (Figure 2). To isolate drug-specific effects, we used a GTP analogue, guanosine-5′-[(α,β)-methylene]triphosphate (GMPCPP), which compared to GTP is hydrolyzed at

[2] http://pymol.sourceforge.net.

[3] www.accelrys.com.

[4] http://visone.info.

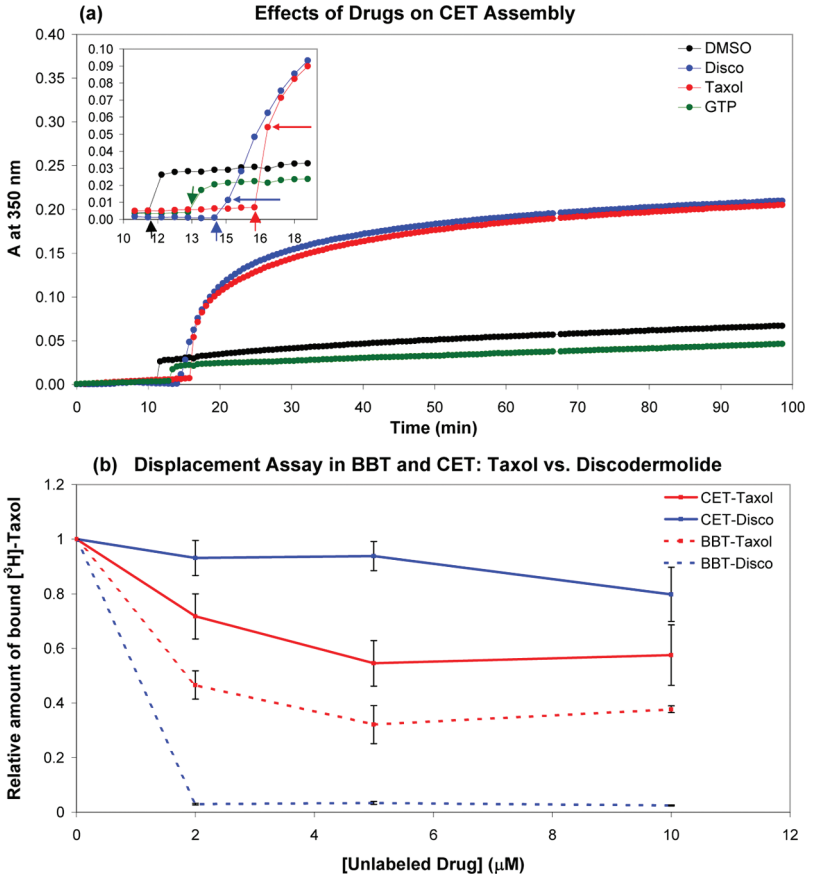

FIGURE 1: Effects of Taxol and discodermolide on CET assembly (a) and drug displacement assays in CET and BBT (b). (a) *In vitro* activities of Taxol and discodermolide using a tubulin polymerization assay. Purified chicken tubulin, stored in a GTP-containing buffer, was diluted to 8 μM in 0.5 M MEM buffer containing 3 M glycerol. The mixture was incubated at 37 °C until the absorbance at 350 nm reached a plateau, at which time DMSO (control), 8 μM GTP, and 8 μM drug was added sequentially, and the absorbance was followed for 80 min. The inset is an enlargement of the time frame immediately before, during, and after drug addition. Thick short vertical arrows point toward the time of addition, while thin horizontal arrows indicate the time point immediately after. (b) Displacement analyses were performed as described in Materials and Methods. Microtubules were assembled in the presence of different concentrations of nonradioactive Taxol or discodermolide and GTP before addition of [^{3}H]Taxol. The amount of tritiated drug, relative to control (0 μM unlabeled drug), was determined. Displacement curves for CET are shown as solid lines, and those for BBT are dashed.

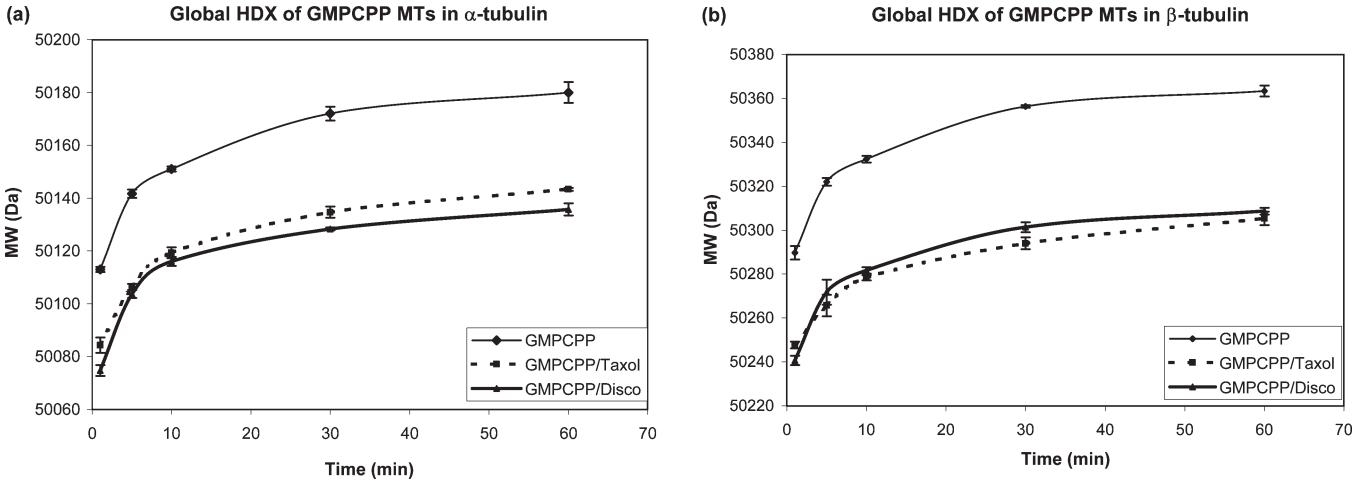

FIGURE 2: Global hydrogen−deuterium exchange for chicken α- (a) and β-tubulin (b) in the presence of GMPCPP alone (control), with Taxol, or with discodermolide. Using HPLC coupled to a LTQ mass spectrometer, the molecular weight of tubulin preincubated with GMPCPP/DMSO or GMPCPP/drug was measured at five different time points after further incubation at 37 °C in deuterated 0.1 M MEM buffer.

an extremely slow rate (*34*). Owing to its very slowly hydrolyzable nature, GMPCPP produces very stable microtubules (*34*), forming a skeleton against which ligand-specific effects can be accurately assessed. GMPCPP-tubulin incubated in the presence of DMSO was used as a control and exhibited a significantly greater extent of deuterium incorporation than the drug-bound tubulin (Figure 2). The overall extent of deuteration was very similar for Taxol and discodermolide (Figure 2).

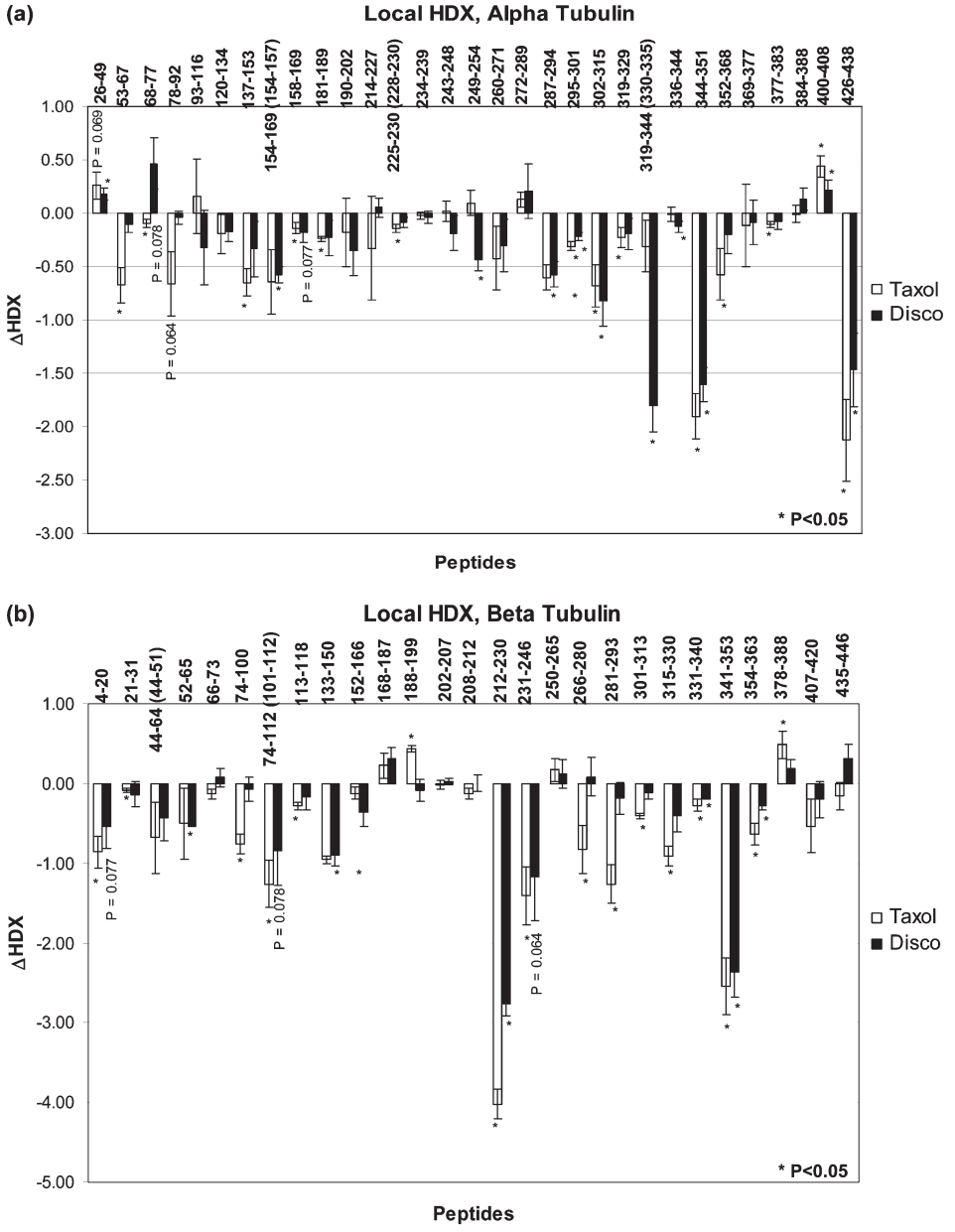

FIGURE 3: Drug-induced alterations in deuteration referenced against GMPCPP-stabilized microtubules for (a) α-tubulin and (b) β-tubulin. Data indicate the mean ± standard deviation of three separate experiments. Differences in deuteration (ΔHDX) are expressed as mass units. For overlapping peptides, unique residues are indicated in parentheses. All peptides with significant alterations in deuterium incorporation ($P < 0.05$) are marked with an asterisk. Some relevant peptides with average ΔHDX values just outside the significance level are labeled with their respective P values.

Local HDX in Specific Regions of the Microtubule. Global View. Although the results of global HDX showed only slight difference between the overall levels of deuterium incorporation in the presence of Taxol as compared to discodermolide (Figure 2), we proceeded to obtain more detailed region-specific deuteration data, as the effects of the two drugs could differ at the various interfaces of the microtubules. Since deuterium labeling reached a near-plateau after 30 min of incubation (Figure 2), we selected this time point for the local experiments. After preincubation in the presence of GMPCPP, CET was further incubated with DMSO (control), Taxol, or discodermolide, subjected to HDX for 30 min, quenched with pH 2.5 denaturing phosphate buffer in a chilled ice bath, and immediately digested with equimolar pepsin in solution (pH 2.1) for 5 min on ice. The resulting peptides were separated by HPLC followed by mass spectrometry analysis.

A 12 T FT-ICR MS equipped with TriVersa NanoMate detected 35 α- and 40 β-tubulin overlapping peptides, produced by pepsin digestion, resulting in an overall sequence coverage of 91% and 93%, respectively. During the HDX experiments these values decreased to 80% each, due to the broadening of some mass peaks caused by partial deuterium incorporation. Supporting Information Figure S3 shows representative spectra for one α- (α287−294, H9) and one β-tubulin peptide (β341−353, loop S9). Panels a and b of Figure 3 compare the effects of Taxol and discodermolide on deuterium labeling in individual peptides of α-tubulin and β-tubulin, respectively. For overlapping peptides the unique residues were indicated in parentheses. Peptides that exhibit significant changes in deuterium incorporation were mapped onto the tubulin dimer structure (1JFF, Figure 4).

Interprotofilament Region. Contacts between the residues in the M-loop (residues 274−288) and the N-terminal H1−S2

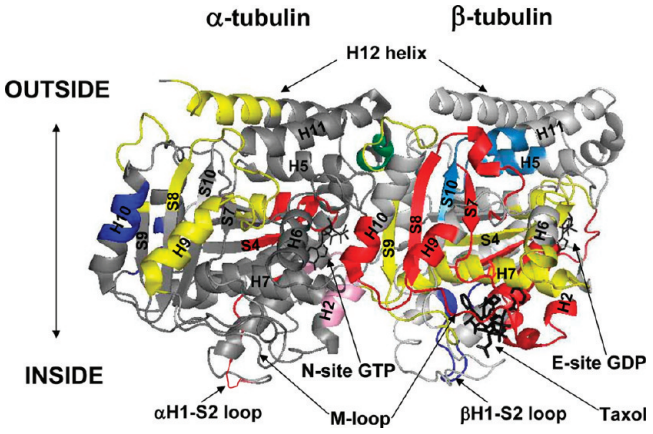

FIGURE 4: Mapping the differences and similarities between the local HDX profiles of Taxol- and discodermolide-bound microtubules (1JFF). The peptides are color-coded as follows: dark blue = discodermolide is more protective; red = Taxol is more protective; yellow = both drugs provide similar protection; pink = discodermolide is deprotective, while Taxol has no effect; light blue = Taxol is deprotective, while discodermolide has no effect; and green = both drugs provide similar deprotection from deuterium incorporation. Secondary structure designations are shown in black and are based on Nogales et al. (*7*).

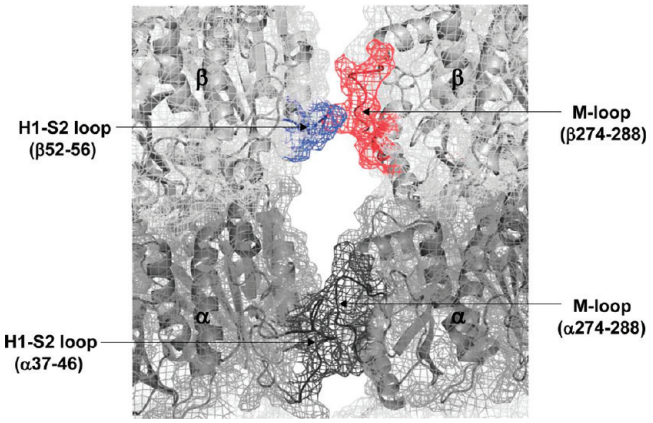

FIGURE 5: Mapping local HDX alterations induced by Taxol and discodermolide on the lateral interprotofilament interface of a previously constructed chicken tubulin model (*12*). Parts of the H1−S2 loop and the M-loop involved in lateral contacts are indicated in parentheses. In black are unaffected regions (αH1−S2 and M-loops). The *β*M-loop, shown in red, is protected from deuteration by Taxol binding but not discodermolide. The *β*H1−S2 loop (blue) shows reduced labeling when discodermolide is bound but not when Taxol is bound.

loop (residues 24−64) of the adjacent protofilament are the major players in forming lateral interactions between the microtubule protofilaments (*35*, *36*). Figure 5 is a visual representation of the lateral contacts and has the exchange data mapped onto a tubulin protofilament pair previously constructed in our laboratory (*12*). In α-tubulin, neither the M-loop nor the H1−S2 loop is protected from deuterium incorporation by either Taxol or discodermolide. In *β*-tubulin, the M-loop (peptides *β*266−280 and *β*281−293) is very strongly protected by Taxol (ΔHDX = −0.82 and −1.26, $P < 0.05$) but not at all by discodermolide. The H1−S2 loop is slightly protected by both drugs (*β*44−64 and *β*52−65, Figure 3b). Note, however, that due to a high error limit of the result for Taxol only discodermolide produces a significant ($P < 0.05$; see Materials and Methods) reduction in labeling at this site.

Interdimer Region. Figure 6a represents the exchange data at the interdimer interface, a region of contact between the

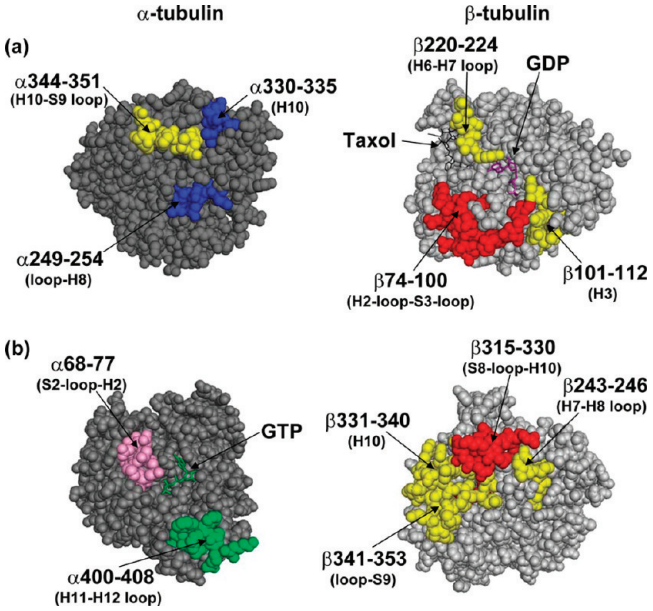

FIGURE 6: Mapping the local HDX alterations on the (a) inter- and (b) intradimer interfaces of the tubulin dimer (1JFF). The peptides are colored according to the code in Figure 4. Briefly, peptic peptides labeled in blue are more protected by discodermolide; in red are more protected by Taxol; in yellow are protected similarly by both drugs; in green are deprotected similarly by both drugs; and in pink are deprotected by discodermolide but unaffected by Taxol. Secondary structure designations are based on Löwe et al. (*8*).

Table 1: Estimated K_d Values for Taxol and Discodermolide in Chicken Erythrocyte Tubulin[a]

	taxane pocket in binding *β*-tubulin		interdimer interface	
	Taxol	Disco	Taxol	Disco
mean − log K_d	5.52	4.10	−3.47	0.85
SD	1.57	0.27	2.14	0.58
K_d (M)	3.04×10^{-6}	**8.00×10^{-5}**	2979	**0.14**

[a]Taxol and discodermolide were docked into the taxane binding pocket in *β*-tubulin and into the interdimer interface of the previously developed protein structure model of chicken erythrocyte tubulin (*12*) using the SURFLEX program (*30*). The −log K_d values for the ten top-scoring results were obtained, and the averages and standard deviations are reported here. The estimated K_d values were derived from the corresponding −log K_d. The values highlighted in bold suggest that discodermolide is much more likely to bind to the *β*-tubulin binding site than the interdimer interface, as the predicted K_d for the former region is over 1000-fold higher than the K_d for the latter.

adjacent α*β*-dimers along the length of the protofilament. Secondary structure designations are made on the basis of the map in Löwe et al. (*8*). There is extensive reduction of deuterium incorporation in this region by both Taxol and discodermolide, as evidenced by three peptides on both α- and *β*-tubulin. Taxol is particularly effective at protecting the *β*-tubulin face of the interdimer region from exchange, as represented by peptides *β*74−100 (H2−loop−S3−loop), *β*101−112 (H3), and *β*220−224 (H6−H7 loop). The respective ΔHDX values were −0.76, −1.26, and −4.02 (Figure 3). Discodermolide, on the other hand, while protective of the latter two peptides on *β*-tubulin (ΔHDX = −0.84 and −2.76), reduces deuterium incorporation on the α-tubulin face of the interdimer region to a greater extent, as represented by its unique protection of peptides α330−335 (part of H10) and α249−254 (loop−H8). The average ΔHDX values

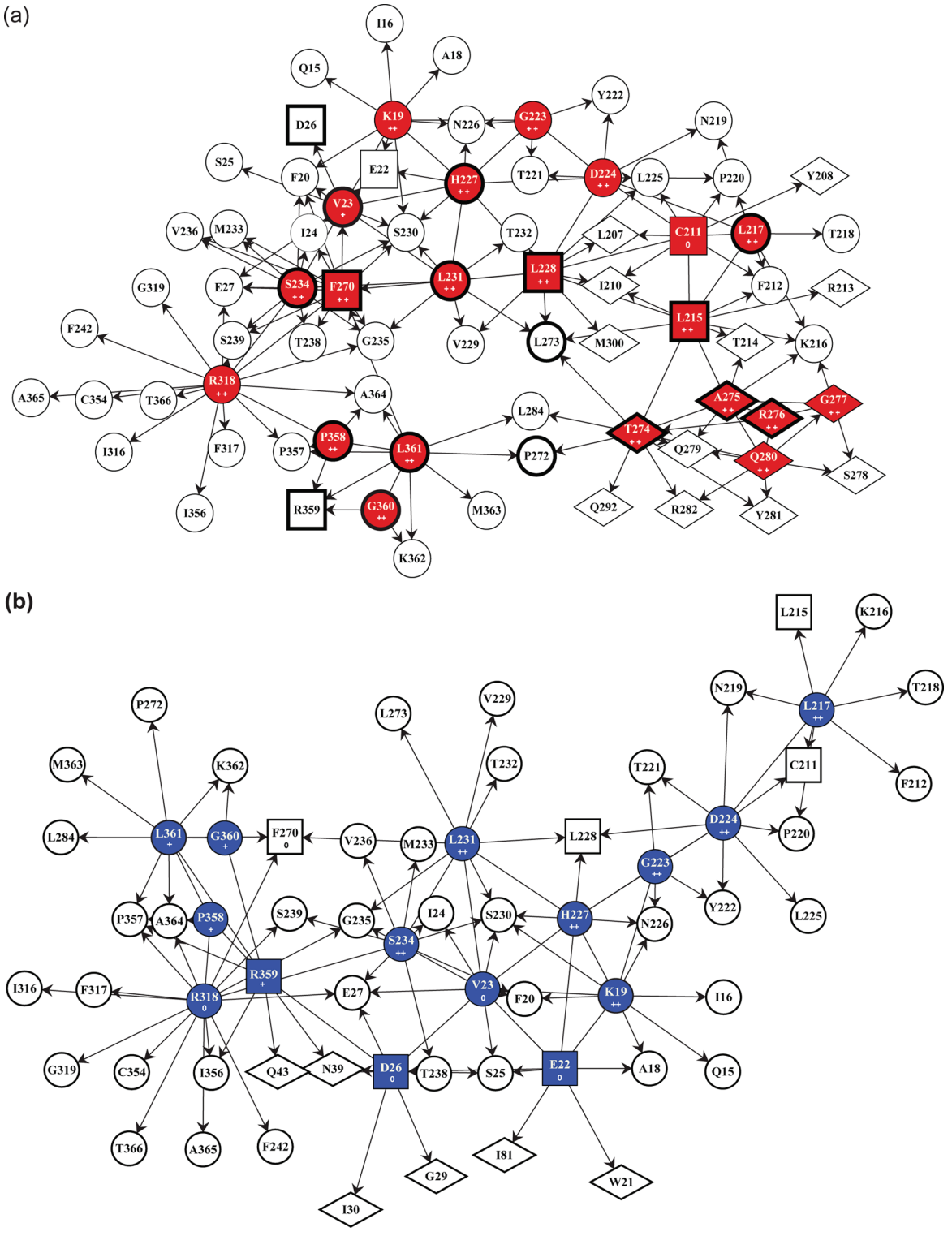

FIGURE 7: Contact maps of Taxol (a) and discodermolide (b) with chicken erythrocyte tubulin. In color (red for Taxol and blue for discodermolide) are the residues in β-tubulin that make primary contacts with the corresponding drug. Clear shapes represent secondary contacts, those that interact with primary ones, but not the drug itself. Residues in squares are represented in both contact maps but as primary contacts in one and secondary in the other. Residues in diamonds are unique to the corresponding drug. Those in circles are shared between the two drugs. Plusses and zeros are used to designate correspondence with changes in HDX of peptides containing the indicated amino acid residues: ++ indicates a large significant decrease in labeling (ΔHDX > 0.5), + indicates a small but significant decrease in labeling (ΔHDX > 0), and 0 indicates no effect on labeling (ΔHDX $= 0$). In (a), residues that have been previously shown to interact with Taxol are boxed in bold (*8*).

for discodermolide and these peptides were -1.80 and -0.44, respectively, while for Taxol they were -0.31 and $+0.10$. The two drugs induce similar reductions in deuteration of peptide 344−351 (H10−S9 loop) in α-tubulin ($\Delta HDX_{Disco} = -1.60$ and $\Delta HDX_{Taxol} = -1.90$).

The exchangeable nucleotide binding site (E-site) in β-tubulin was well protected from deuterium incorporation by both Taxol and discodermolide, as can be seen from significant reduction in labeling of peptide β133−150 ($\Delta HDX_{Taxol} = -0.95$, $\Delta HDX_{Disco} = -0.89$) and a slight reduction in peptide β4−20 (Figure 3b). The former

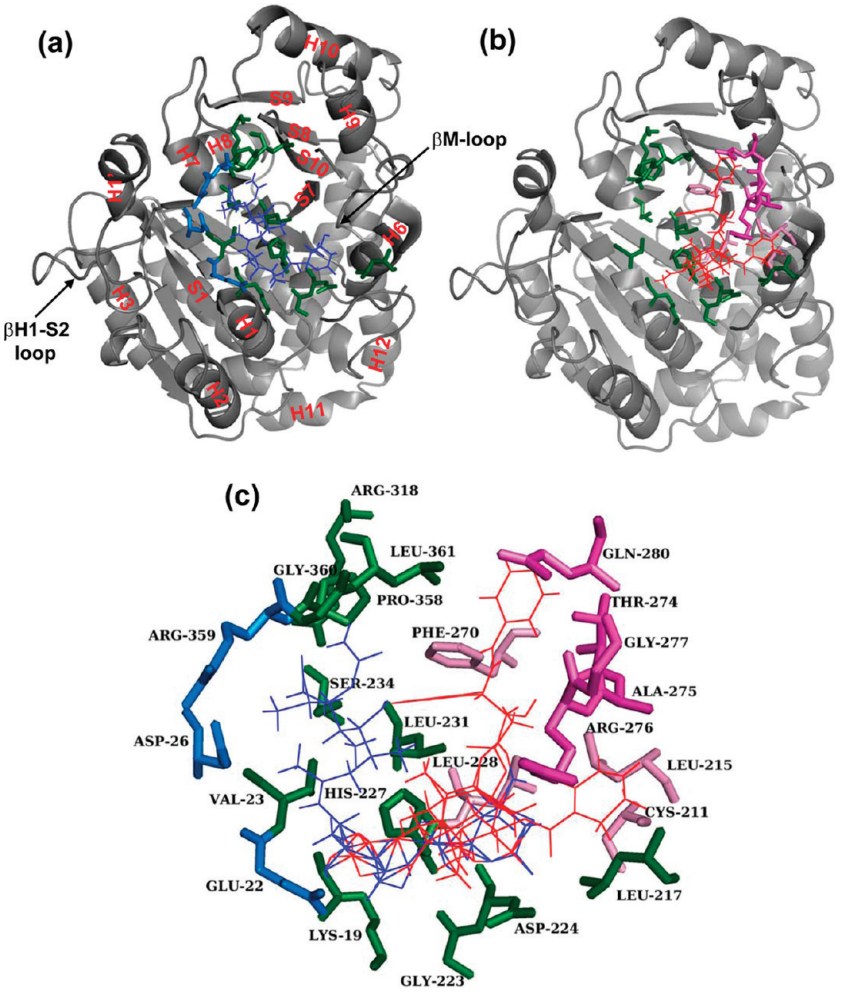

FIGURE 8: Structural representation of the discodermolide and Taxol binding sites. Shown in gray and in the same orientation are cartoon representations of the β-tubulin taxane binding pocket with docked discodermolide (a) and Taxol (b). In (a) all secondary structure designations are labeled in red and are based on Löwe et al. (*8*). In all parts of the figure (a−c) docked Taxol is shown in red and discodermolide in blue. Amino acids that form direct contacts with both drugs are shown in green (colored circles in Figure 7). In blue are the amino acids that make unique interactions with discodermolide (blue squares in Figure 7b). Residues that make unique contacts with Taxol and are part of the M-loop (red diamonds in Figure 7a) are shown in magenta, while those outside the M-loop (red squares in Figure 7a) are in light pink.

contains residues that come in direct contact with the GMPCPP phosphates, while the latter is involved in interactions with both the base and the phosphates (*8*).

Intradimer Region. Figure 6b represents the exchange data at the intradimer interface, a region of contact between α- and β-tubulin monomers within a dimer pair. Peptide 400−408 in α-tubulin (H11−H12 loop) is slightly deprotected by both Taxol and discodermolide. Corresponding peptide in β-tubulin, β250−265 (H8, not shown), which interacts with α400−408, is not affected by either drug. Peptide α68−77 (S2−loop−H2) is slightly protected from deuterium incorporation by Taxol but is deprotected in the presence of discodermolide. The peptide on β-tubulin that interacts with α68−77, β243−246 (H7−H8 loop) is well shielded by both drugs. However, since β243−246 is part of a larger peptide that was detected in the HDX experiments (β231−246; see Figure 3b), which also contains residues involved in direct interaction with both drugs (see results below), it is possible that this specific region is also unaffected by the binding of Taxol and discodermolide, as is its α-tubulin counterpart.

Unlike the α-tubulin face of the intradimer region, β-tubulin is well protected by both drugs. Peptide β341−353 (loop−S9) is highly protected from deuterium incorporation (ΔHDX_{Taxol} = −2.55, ΔHDX_{Disco} = −2.37, Figure 3), second only to the residues in the taxane binding site. Although to a much smaller extent (ΔHDX_{Taxol} = −0.23, ΔHDX_{Disco} = −0.18), the labeling of residues β331−340 (H10) is also reduced by the binding of both Taxol and discodermolide. Taxol provides additional protection from deuteration on the β-tubulin face of the interdimer region, as significant reduction in labeling with an average ΔHDX value of −0.91 is observed for peptide β315−330 (S8−loop−H10). Discodermolide may lack this effect on β315−330 since the obtained decrease in deuterium incorporation was not statistically significant ($P < 0.05$), as defined by a two-tailed *t*-test (see Materials and Methods).

Peptide α137−153 (S4−loop−H4) undergoes a decrease in labeling upon Taxol binding (Figure 3a) and is immediately adjacent to the phosphates of GTP in the nonexchangeable binding site (N-site) in α-tubulin (*8*). The effects of discodermolide on the labeling of this peptide are not significant. Overall, the residues in the N-site are considerably less protected from deuterium incorporation by the binding of either drug than those at the E-site.

MAP Binding Site. Helix H12 (residues 415−434), known to play a major role in the binding of motor proteins, kinesin and dynein (*37*), as well as microtubule-associated proteins (MAPs), such as tau and MAP2 (*38*), exhibits reduced labeling in α-tubulin

Amino Acid Residues	Atoms in Discodermolide (number of contacts)								
K19	C8								
E22	C8	C9	**C11-OH**	C2 (2)					
V23	C13	C20	C23	C24	C28	C31	C32		
D26	C13 (2)	C29	C32 (2)						
L217	C1	C2	C25 (4)						
G223	C8								
D224	*C1* (3)	*C1-O (lactone)*	**C1=O**	*C5*	**C7-OH**	C26 (2)			
H227	*C3*	C4 (2)	C5	C6	*C7 (3)*	C8 (2)	*C17-OH*	C30	C31
L231	C4	C24 (2)	C26	C31 (2)					
S234	C24								
P358	C22 (2)	C24	$C_{carbamate}$	*N carbamate*					
R359	C21	C29	C32						
G360	*C17*	*C17-OH*	*C19*	**$N_{carbamate}$** (2)					
L361	*C carbamate* (2)	**$N_{carbamate}$**							

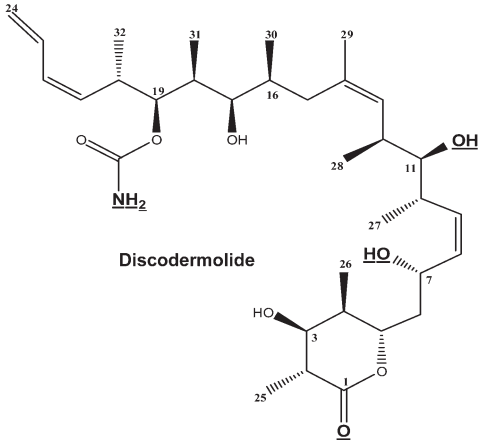

FIGURE 9: Specific interactions of discodermolide with β-tubulin isolated from chicken erythrocytes. The table lists specific contacts made between the residues in the β-tubulin taxane binding pocket (Figures 7b and 8c) and the atoms in discodermolide. In parentheses is the number of contacts formed between the specified atom and the corresponding amino acid. In bold are the atoms that form hydrogen bonds with the corresponding amino acids in β-tubulin. The moieties involved in hydrogen bond formation are also bold and underlined in the structural representation of discodermolide. In italics are the discodermolide atoms that make either van der Waals or polar contacts with the corresponding residues in β-tubulin. The rest are hydrophobic interactions.

when either Taxol or discodermolide is bound (Figure 3a, peptide α426−438). H12 in β-tubulin was not detected in our exchange experiments.

Drug Binding Sites. For both Taxol and discodermolide, the largest reduction in labeling in the data set is found in the H6−H7 loop (β212−230) with smaller changes at the core helix βH7 (β231−246). Together, these two regions have been shown to stabilize the 2-phenyl ring of Taxol (*8*). Leu217 has also been implicated in making van der Waals contacts with discodermolide (*25*). Helix H1 (β4−20), involved in stabilization of the 3′-phenyl ring and the *N*′-phenyl of Taxol, exhibits significantly reduced labeling in the presence of Taxol. Discodermolide, although never before shown to interact with this region, provides some protection, slightly outside the significance level (P = 0.077). Loop S9−S10 (β354−363) shows small, but significant reduction in labeling in the presence of both drugs, with Taxol having a stronger effect than discodermolide. This loop was shown to be in close contact with Taxol (*8*). Additionally, in our previous studies with photolabeled discodermolide analogues, residues 355−360, that are part of the S9−S10 loop, were specifically labeled with C19-BPC-discodermolide (*24*).

Finally, as was mentioned in the context of lateral interactions, the M-loop (β274−288) is highly protected by Taxol but not by discodermolide. Previously, the oxetane ring of Taxol was shown to interact with the M-loop of β-tubulin (*8*), and contacts with this region were reported for discodermolide in tubulin isolated from bovine brain (*24*, *25*). In our study, however, the significant difference in the labeling of the M-loop between Taxol and discodermolide suggests distinct orientations for the two drugs in the β-tubulin binding pocket (see Discussion below).

Computational Docking of Discodermolide. Based on the local HDX profile (Figure 3), the most likely binding site for discodermolide was in β-tubulin, in the same pocket as Taxol, since the regions with the most labeling reduction due to discodermolide binding were within the taxane binding pocket with the exception of the M-loop. The interdimer region, however, could not be excluded on the basis of the exchange data. Therefore, discodermolide was computationally docked in its natural and disk-shaped (*25*) conformations into the β-tubulin luminal binding pocket (excluding the M-loop) and into the interdimer interface.

Since the results produced with the disk-shaped discodermolide were not consistent with the HDX data (Figure 3), this drug conformation was excluded from playing a role in the binding of CET. Interdimer interface was excluded as a possible binding site for discodermolide because the docking experiments predicted its K_d to be over 1000-fold higher than the K_d for the β-tubulin luminal binding pocket (Table 1).

Finally, docking discodermolide in its natural conformation into the taxane binding pocket in β-tubulin produced a contact map that was both consistent with the exchange data and provided an explanation of the displacement assay between Taxol and discodermolide (Figure 1b). Figure 7 illustrates the contacts made by Taxol (a) and discodermolide (b) in the

β-tubulin binding site. Although many primary (direct) contacts are shared (red or blue circles), each drug forms unique interactions with residues in the binding pocket (red or blue squares and diamonds). Similarly, secondary contacts, those interacting with primary residues but not with either of the drugs themselves, are largely shared between Taxol and discodermolide (white circles), but there are a number of distinctive ones (white squares and diamonds). In Figure 8c it is clearly shown that Taxol (red) and discodermolide (blue) overlap in the taxane binding site, but the binding pose of these drugs within this pocket is distinct for each of the two drugs. While Taxol is oriented toward the M-loop (Figure 8a), discodermolide is rotated away from it and toward the N-terminal residues Asp26 and Glu22 (Figure 8b).

The majority of the contacts made between discodermolide and the residues in the β-tubulin taxane binding pocket are hydrophobic (Figure 9). There are a number of van der Waals and/or polar contacts (shown in italics in Figure 9). The two types of contacts could not be distinguished by the docking software. Most importantly, there are five defined hydrogen bonds (bold in Figure 9) formed between the carbamate nitrogen of discodermolide and Leu361, the carbamate nitrogen and Gly360, the C1 ester carbonyl and Asp224, the C7 hydroxyl and Asp224, and the C11 hydroxyl and Glu22. The last of the five is a unique contact between discodermolide and β-tubulin and is not formed with Taxol.

DISCUSSION

Mode of Microtubule Stabilization by Discodermolide. Overall, in the presence of GTP, which is analogous to both the physiological conditions and the conditions used in our HDX experiments, the effects of Taxol and discodermolide on chicken erythrocyte tubulin (CET) polymerization were very similar. In the assembly assay, discodermolide induced polymer formation to the same extent as Taxol. However, the ability of discodermolide to nucleate microtubules was weaker than that of Taxol, as suggested by a lower absorbance immediately after drug addition and the initial rate of polymerization. The opposite effect is observed in tubulin isolated from calf brain: not only does discodermolide induce more polymerization than Taxol, but it also exhibits a much greater nucleation potential (*14*). Similarly unexpected were the results of the displacement studies between Taxol and discodermolide in CET, in which Taxol was able to displace discodermolide, even at one-fifth the concentration of the competing drug, which is the opposite of what has previously been shown (*17*, *24*, *33*) and what we observe from the displacement studies with BBT, where discodermolide has a much greater affinity for tubulin than Taxol and is able to displace Taxol from the MTs. It has also been demonstrated with BBT that Taxol and discodermolide have the ability to induce MT assembly even in the absence of GTP, which is normally required for polymerization (*3*, *14*). Under these conditions, however, unlike tubulin isolated from the bovine brain, CET is polymerized faster and to a much greater extent in the presence of Taxol than in the presence of discodermolide (Supporting Information Figure S2). Therefore, the results of our displacement and assembly studies with CET suggest one of two possibilities: either discodermolide has an alternative binding site from Taxol or it binds in the taxane pocket in β-tubulin with a weaker affinity. Additionally, our results highlight the importance of the role played by tubulin isotypes in determining drug sensitivity, as the major difference between bovine brain and chicken erythrocyte tubulin is the isotype composition. While chicken erythrocyte tubulin contains only one α1 and one βVI tubulin isotype, bovine brain is composed of more than one α- and four β-tubulin isotypes, βI−IV. As neither of the tubulin sources is human, it is unclear which one best approximates the effects of the drugs on human tubulin. For example, given the *in vitro* effects of discodermolide on bovine brain tubulin, one would expect this drug to be more cytotoxic to cells, yet its IC_{50} in a number of human cell lines is higher than that of Taxol (*17*, *22*). These observations are more consistent with our *in vitro* studies in chicken erythrocyte tubulin. It is therefore of equal relevance to study the conformational effects of the microtubule stabilizing agents in tubulin originating from different sources and composed of different isotypes.

Consistent with the observation that discodermolide and Taxol induce the same extent of polymerization in the presence of a trinucleotide, overall reduction in labeling of tubulin was also similar for both drugs, but much lower than that in the control GMPCPP-MTs. This implies that Taxol and discodermolide most probably share the same binding site. If discodermolide were to bind at an alternative site, both the overall and the region-specific stabilization of tubulin would be expected to differ significantly from that induced by Taxol. The results of local HDX experiments that afforded region-specific information further confirmed significant overlap in protection of residues both in- and outside the taxane binding site in the lumen of β-tubulin, with some small but significant regional differences.

Neither Taxol nor discodermolide provides lateral stabilization in α-tubulin, as the main regions involved in interprotofilament contacts, the M-loop and the N-terminal H1−S2 loop, are not protected from deuterium incorporation by either drug. In β-tubulin, on the other hand, Taxol imparts significant protection on the M-loop (represented by peptides β266−280 and β281−293), while discodermolide has no effect. This effect of Taxol is consistent with previous HDX studies (*12*, *39*). Since the M-loop is also a relevant component of the taxane binding pocket and makes direct contacts with the Taxol molecule (*8*)(−*11*), the observed differences in labeling between the two drugs suggest that if discodermolide does in fact bind at this site, its orientation inside the pocket is distinct from that of Taxol. This is further addressed below, in the discussion of the results of the docking experiments with discodermolide. The region complementary to the M-loop, βH1−S2 loop (β52−65), is protected by both Taxol and discodermolide, with the former drug resulting in a reduction in labeling that is slightly outside the defined statistical significance ($P < 0.05$). Therefore, we can only claim with confidence that discodermolide imparts stability on this region, while the effects of Taxol are of unknown significance. The results with Taxol are consistent with those reported in our earlier studies (*12*) and with predictions made by Keskin et al. using a computational approach (*40*), such that most of the stabilization of lateral contacts by this drug occurs in the near vicinity of its binding to β-tubulin. This further highlights the accuracy of the obtained HDX data. More importantly, discodermolide appears to have a similar effect as Taxol, as its stabilization of lateral interactions is due to residues in the N-terminal region of β-tubulin, which is implicated in its binding (see discussion below), but not due to the M-loop. Thus, the stabilization of interprotofilament interactions due to the MSAs that bind to the taxane pocket in β-tubulin seems to be the direct effect of the drugs' primary contacts with the residues of the lateral interface.

On the interdimer interface, discodermolide provides significant stabilization, particularly on the α-tubulin face of the region,

as evidenced by significantly reduced labeling of peptides α249−254 and α330−335 (Figure 6a). The major effects of Taxol in this region are seen on the β-tubulin face and only to a small degree on the side of α-tubulin, which underscores its strong conformational effects on the subunit to which it binds.

Taken together, the results for the interdimer and lateral interfaces suggest complementary actions of Taxol and discodermolide on MT stabilization, which may provide a molecular basis for the observed *in vivo* synergy between the two drugs (*20*, *22*). While Taxol has strong stabilizing effects on the β-tubulin side of the interdimer interface and on the M-loop involved in lateral contacts, discodermolide shows significant protection of the complementary regions, the α-tubulin face of the interdimer region and the N-terminal βH1−S2 loop, respectively. Although there has not been any evidence from *in vitro* studies that there is synergy at the level of MTs, the assay used to assess this, i.e. microtubule assembly, may not be sufficiently sensitive to detect synergistic effects at the molecular level. In other words, the extent of polymerization may not fully describe functional capabilities and stability of the assembled MTs, while fine changes in the conformation, such as those detected in our study, provide a much more accurate description of the complementary molecular effects of the drugs.

At the intradimer interface, stability is induced by both drugs (Figure 6b). Helix H10 and the H10−S9 loop in β-tubulin are protected significantly from deuterium incorporation when either Taxol or discodermolide is bound. The corresponding region across the interface, αT5 loop (α170−180), was not identified in our experiments, most likely due to its apparently low abundance under the applied conditions. Unlike discodermolide, Taxol stabilizes the βS8−loop−H10 region, whose α-tubulin partner (α214−227) lacks significant protection when either of the drugs is present, which suggests that the β-tubulin peptide moves to preclude solvent access to itself without affecting exchange at the corresponding α-tubulin site. In α-tubulin, the H11−H12 loop is slightly deprotected by both Taxol and discodermolide, suggesting that it moves outward to face the surface of the microtubule where it becomes more accessible to deuterated solvent. One significant difference between the two drugs is in their effects on peptide α68−77 (S2−loop−H2). While Taxol has a very small protective effect on this region, discodermolide leads to its deprotection. Residues on β-tubulin that interact with α68−77 across the interface are 243−246 and are part of a larger identified peptic peptide β231−246. As mentioned in the results above, this region is highly protected by both Taxol and discodermolide, which is most likely due to the residues that directly interact with the drugs and are not part of the smaller region at the intradimer interface. Therefore, it is possible that amino acids β243−246 are not protected from deuteration by either or both drugs. However, due to insufficient resolution, this claim cannot be made in complete confidence. Overall, we see increased stabilization of the intradimer interface, but to a lesser extent than the interdimer region. Discodermolide, however, is less effective at providing stability at the intradimer interface than Taxol, as evidenced by a region of deprotection from deuterium incorporation on the α-tubulin side of the interface due to the binding of discodermolide and an additional place of protection by Taxol on β-tubulin.

The exchangeable nucleotide binding site (E-site) was equally well protected from deuteration by both drugs, as represented by reduced labeling in peptides β4−20 (S1−loop−H1) and β133−150 (S4−loop−H4) that are involved in interactions with the nucleotide base and the phosphates of, in our case, GMPCPP. In addition, discodermolide exhibits unique protection of a region in α-tubulin (α249−254) that contains an amino acid, namely, Glu254, which is involved in hydrolyzing GTP (*41*). This suggests that not only does discodermolide induce the tightening and stabilization of GTP binding in the E-site, but also it may hinder hydrolysis in the tubulin subunits whose GTP has not yet been hydrolyzed, namely, the GTP-cap at the (+)-end of the microtubules, thereby imparting additional stability to the whole MT structure. This possibility will be further investigated in our future experiments and may shed some light onto the microtubule nucleation versus elongation power of discodermolide compared to Taxol.

The nonexchangeable nucleotide binding site (N-site) is considerably less protected by the drugs. Taxol has a small, but significant shielding effect on residues α137−153 (S4−loop−H4) that are involved in the stabilization of the nucleotide phosphates, while discodermolide does not.

Effects on Binding of Endogenous Proteins. Both Taxol and discodermolide stabilize the H12 helix of α-tubulin, as the labeling of the corresponding peptide (α426−438) was significantly reduced when either drug was bound to the MTs. Helix H12 has been previously shown to bind motor proteins, kinesin and dynein (*37*), as well as MAPs, such as tau and MAP2 (*38*). The protection of this region by the binding of Taxol and discodermolide suggests that these drugs modulate the interactions between MTs and these endogenous proteins. In fact, previous studies have demonstrated that tau has reduced binding to MTs in the presence of discodermolide (*42*) and a different binding site in the presence and absence of Taxol (*43*). Interactions of microtubules with any other endogenous proteins that may bind the C-terminal region of tubulin can potentially be similarly affected by this drug-induced stabilization of the H12 helix. This may have important implications in downstream signaling involving these microtubule binding proteins.

Exploring Alternative Binding Sites of Discodermolide. The results of the hydrogen−deuterium exchange experiments suggested two possible binding sites for discodermolide, the interdimer interface and the taxane binding pocket in β-tubulin. The reductions in labeling at the former region can be attributed to the allosteric stabilization of the contacts between adjacent dimers in the protofilament, although it cannot be excluded as an alternative binding site. In addition, based on NMR experiments it was proposed that when bound to microtubules discodermolide assumes a disk-shaped conformation (*25*). Thus, both unaltered and disk-shaped discodermolide were docked into the two aforementioned sites using flexible-ligand data-directed docking simulations with Taxol serving as a control. Contacts predicted from the docking experiments with the disk-shaped discodermolide were not consistent with the exchange data, which allowed us to eliminate this conformation.

Docking of discodermolide at the interdimer interface in its unaltered conformation resulted in an estimated K_d that was over 1000-fold higher than that for the β-tubulin binding pocket (Table 1). Although absolute values of K_d determined from the docking experiments are not good measures for the real K_d values, they provide a strong and reliable tool for comparing relative affinities of ligands for the different sites within a target protein. Confirmation of this comes from our finding that Taxol has a much lower estimated K_d for the taxane pocket of β-tubulin than for the interdimer interface, as is expected since the luminal pocket in β-tubulin is a known binding site for Taxol.

Although the contact map generated for discodermolide in the interdimer interface matched well with the exchange data, the

number of interactions made with the residues in this region (data not shown) was significantly lower than that in β-tubulin (6 vs 15), which is consistent with the estimated higher K_d value for the binding at the interdimer interface. Therefore, the β-tubulin site is a much more likely place for discodermolide to bind than the interdimer region.

Major reductions in labeling due to the binding of discodermolide were observed in peptides that comprise the taxane binding site, with the exception of the M-loop (β274−288). Taxol, on the other hand, induced significant reduction in labeling in the β-tubulin M-loop, which is consistent with previous determinations of contacts made by Taxol in the taxane binding site (*8*). This difference between the two drugs allowed us to unequivocally exclude the M-loop from being involved in interactions with discodermolide in its binding site. The docking simulations of discodermolide in the taxane binding pocket resulted in 20 possible conformations of the drug. Although the discodermolide poses that interacted with the M-loop had comparable K_d values to those that did not, they were excluded on the basis of the aforementioned HDX results. This led to an identification of a distinct binding orientation for discodermolide in the taxane binding pocket.

There is significant overlap between Taxol and discodermolide within the luminal binding pocket in β-tubulin (Figures 7 and 8c). Lys19, Val23, Leu217, Gly223, Asp224, His227, Leu231, Ser234, Arg318, Pro358, Gly360, and Leu361 all make direct contacts with both drugs. All but four of these residues (Lys19, Gly223, Asp224, and Arg318) were previously shown to interact with Taxol directly (*8*). Moreover, identification of residues Pro358, Gly360, and Gly361 as primary contacts for discodermolide is consistent with our previous studies, where a photoaffinity-labeled analogue of discodermolide, C19-[^{3}H]BPC-discodermolide, specifically bound to peptide 355−359 in the S9−S10 loop of β-tubulin (*24*). One of the unique primary contacts made with discodermolide was Arg359, which is also part of the aforementioned peptide and further adds to the validity of our results. Other distinct contacts made with discodermolide were with the residues in the N-terminal H1−S2 loop, namely, Glu22 and Asp26. This, in addition to the fact that, consistent with previous findings (*8*), the main unique primary contacts of Taxol were all in the βM-loop (Thr274, Ala275, Arg276, Gly277, and Gln280), suggests that discodermolide orients itself away from the M-loop and toward the H1−S2 loop on the opposite side of the taxane binding pocket.

Amino acids Cys211, Leu215, Leu228, and Phe270 directly interact with Taxol but are only secondary contacts for discodermolide, those that interact with primary (direct) contacts, but not the drug itself. Ovarian cancer cell lines containing a tubulin mutation Phe270Val were shown to have resistance to Taxol but remained sensitive to discodermolide (*17*). This is consistent with our results, since Phe270 is a primary contact for Taxol and is only remotely affected by discodermolide binding.

The N-terminal H1−S2 loop, toward which the discodermolide binding site extends, is second only to the C-terminus in sequence divergence among different β-tubulin isotypes. Comparing the sequences of chicken erythrocyte βVI-tubulin and the major bovine brain βII-tubulin in this region (Supporting Information Figure S1), 31% of amino acids were found to be divergent, with the most significant being residues 32, 37, and 55, which are Ile, Cys, and Tyr in CET and Pro, His, and Thr in BBT, respectively. The next least conserved residues that may have additional effects on tubulin function and drug binding are 35 (N_{CET}→S_{BBT}), 41 (S→D), 56 (S→G), and 57 (H→N). The M-loop, which is directly involved in Taxol binding, but not discodermolide, contains only two spots of divergence, namely, residues A275S and S285T, the latter of which is insignificant, especially since it is not in direct contact with the Taxol molecule. On the other hand, change from an Ala in CET to a Ser in BBT at residue 275, although only a matter of a hydroxide group, can have significant consequences for Taxol binding, as it is a unique primary contact (see Figure 7a). It has been computationally predicted that lack of Ser at position 275 leads to reduced binding of Taxol to the β-tubulin luminal pocket, as this Ser residue is implicated in forming a hydrogen bond with Taxol at its proposed intermediate binding site (*44*). Given the results of our drug displacement studies, it is unlikely that Ser275 is the singular driving force for Taxol binding. Although we do not have the exact K_d values for Taxol binding to CET, we know from our experiments that Taxol is unable to displace discodermolide from bovine brain MTs where amino acid 275 is a Ser, while it does so quite efficiently in CET where residue 275 is an Ala. It is therefore unlikely that a single residue can be fully responsible for a drug effect or lack thereof. Microenvironments composed of small groups of amino acids may play a more significant role, such that substitution of one amino acid may compensate for or add to the effect of another residue in the group. Upon further examination of all primary contacts formed with Taxol and discodermolide, we found that all but one amino acid was conserved across the different β-tubulin isotypes. Leu231 is a shared primary contact between Taxol and discodermolide and is an Ala in major bovine and human β-tubulin isotypes. To assess how this difference may affect the binding of Taxol and discodermolide to CET, theoretical −log K_d values of each drug for the taxane binding pocket were obtained via docking simulations and compared for wild-type CET and Leu231Ala CET (data not shown). Mutation of Leu231 to an Ala in CET led to a significant increase ($P < 0.001$) in the computed K_d values, 5-fold for discodermolide and ~150-fold for Taxol. Therefore, this, as well as all of the aforementioned places of sequence divergence between chicken erythrocyte βVI and bovine brain βII-tubulin, can potentially affect the binding modes and affinities of Taxol and discodermolide and offer a possible explanation for the distinct pose of discodermolide in the taxane binding pocket of CET and for the differences observed in the assembly and displacement assay profiles.

Finally, the nature of molecular interactions between discodermolide and β-tubulin in the taxane binding pocket was determined from the results of the docking experiments (Figure 9). The majority of contacts were hydrophobic. Some were either van der Waals and/or polar but could not be resolved with the docking software. Five interactions were classified as hydrogen bonds. These were formed between the carbamate nitrogen of discodermolide and Gly360, the carbamate nitrogen and Leu361, the C1 ester carbonyl and Asp224, the C7 hydroxyl and Asp224, and the C11 hydroxyl and Glu22. The latter of the five hydrogen bonds is a unique contact between discodermolide and β-tubulin and is not formed with Taxol. Moreover, these five bonds span the entire length of the discodermolide molecule, which suggests that the obtained binding conformation is not an artifact of the docking experiments. Thus the detected hydrophobic interactions are most likely genuine binding contacts and not merely the result of proximity. Nonetheless, they seem to be responsible for the protection seen in the local HDX experiments. It is also of note that the proposed binding conformation of

discodermolide is consistent with some of the structure−activity relationship (SAR) studies conducted with discodermolide analogues (*45*). For example, we have shown that a large proportion of interactions is found between tubulin and the linear portion of discodermolide, namely, C16−C24. Truncation of this region in the SAR studies conducted by the Schreiber group led to a loss of cell growth inhibitory activity (*46*). Similarly, any manipulation of the C11 and/or C17 hydroxyl groups was detrimental to biological activity (*45*, *47*). These carbons are both involved in the binding of discodermolide to the taxane pocket, with the former making a hydrogen bond with His227.

In summary, it has been shown that Taxol and discodermolide have very similar effects on microtubule conformation and stability. The region most stabilized by both drugs, other than the binding site, is the interdimer interface, where Taxol exerts most of its effects on the β-tubulin side, whereas discodermolide does this on the α-tubulin side of the interface. The lateral interactions between microtubule protofilaments are also differentially stabilized by the two drugs. Taxol and discodermolide induce stability on the opposite sides of the interprotofilament interface between adjacent β-tubulin subunits, such that those regions that are involved in lateral contacts, the M-loop and the H1−S2 loop, respectively, are also the ones directly interacting with the corresponding drug. These complementary effects of Taxol and discodermolide suggest a possible molecular explanation to the observed *in vivo* synergy between them (*20*, *22*). The intradimer interface is not as well stabilized, and discodermolide has only weak effects in this region. The molecular basis for disruption of interactions between endogenous proteins and the microtubules is thought to be due to unavailability of the C-terminal H12 helix, which occurs as a result of the binding of both Taxol and discodermolide. Finally, discodermolide has a distinct binding orientation inside the taxane binding pocket in β-tubulin, such that the drug is oriented away from the M-loop and toward the H1−S2 loop. Combined with the outcomes of the displacement assay and the GTP-free assembly with CET, which showed that discodermolide is displaced by Taxol from the microtubules and that Taxol induces a much faster assembly and a greater extent of polymer formation than discodermolide, these results suggest that in tubulin isolated from chicken erythrocytes discodermolide binds to the taxane binding site with a weaker affinity than Taxol and highlight the importance of the role played by tubulin isotypes in drug interactions.

ACKNOWLEDGMENT

M.K.-B. gratefully acknowledges C.-P. H. Yang, Ph.D., and B. Burd for guidance with biochemical experiments.

SUPPORTING INFORMATION AVAILABLE

Additional figures showing the alignment of chicken erythrocyte βVI, bovine brain βII, and human βI-tubulin sequences, the GTP-free assembly of CET and BBT in the presence of Taxol and discodermolide, and the representative mass spectrometry data. This material is available free of charge via the Internet at http://pubs.acs.org.

REFERENCES

1. Rowinsky, E. K. (1997) The development and clinical utility of the taxane class of antimicrotubule chemotherapy agents. *Annu. Rev. Med. 48*, 353–374.
2. Rao, S., Horwitz, S. B., and Ringel, I. (1992) Direct photoaffinity labeling of tubulin with taxol. *J. Natl. Cancer Inst. 84*, 785–788.
3. Schiff, P. B., Fant, J., and Horwitz, S. B. (1979) Promotion of microtubule assembly in vitro by taxol. *Nature 277*, 665–667.
4. Rao, S., He, L., Chakravarty, S., Ojima, I., Orr, G. A., and Horwitz, S. B. (1999) Characterization of the Taxol binding site on the microtubule. Identification of Arg(282) in beta-tubulin as the site of photoincorporation of a 7-benzophenone analogue of Taxol. *J. Biol. Chem. 274*, 37990–37994.
5. Rao, S., Krauss, N. E., Heerding, J. M., Swindell, C. S., Ringel, I., Orr, G. A., and Horwitz, S. B. (1994) 3′-(p-azidobenzamido)taxol photolabels the N-terminal 31 amino acids of beta-tubulin. *J. Biol. Chem. 269*, 3132–3134.
6. Rao, S., Orr, G. A., Chaudhary, A. G., Kingston, D. G., and Horwitz, S. B. (1995) Characterization of the taxol binding site on the microtubule. 2-(m-Azidobenzoyl)taxol photolabels a peptide (amino acids 217−231) of beta-tubulin. *J. Biol. Chem. 270*, 20235–20238.
7. Nogales, E., Wolf, S. G., and Downing, K. H. (1998) Structure of the alpha beta tubulin dimer by electron crystallography. *Nature 391*, 199–203.
8. Lowe, J., Li, H., Downing, K. H., and Nogales, E. (2001) Refined structure of alpha beta-tubulin at 3.5 Å resolution. *J. Mol. Biol. 313*, 1045–1057.
9. Ganesh, T., Guza, R. C., Bane, S., Ravindra, R., Shanker, N., Lakdawala, A. S., Snyder, J. P., and Kingston, D. G. (2004) The bioactive Taxol conformation on beta-tubulin: experimental evidence from highly active constrained analogs. *Proc. Natl. Acad. Sci. U.S.A. 101*, 10006–10011.
10. Geney, R., Sun, L., Pera, P., Bernacki, R. J., Xia, S., Horwitz, S. B., Simmerling, C. L., and Ojima, I. (2005) Use of the tubulin bound paclitaxel conformation for structure-based rational drug design. *Chem. Biol. 12*, 339–348.
11. Li, Y., Poliks, B., Cegelski, L., Poliks, M., Gryczynski, Z., Piszczek, G., Jagtap, P. G., Studelska, D. R., Kingston, D. G., Schaefer, J., and Bane, S. (2000) Conformation of microtubule-bound paclitaxel determined by fluorescence spectroscopy and REDOR NMR. *Biochemistry 39*, 281–291.
12. Xiao, H., Verdier-Pinard, P., Fernandez-Fuentes, N., Burd, B., Angeletti, R., Fiser, A., Horwitz, S. B., and Orr, G. A. (2006) Insights into the mechanism of microtubule stabilization by Taxol. *Proc. Natl. Acad. Sci. U.S.A. 103*, 10166–10173.
13. Orr, G. A., Verdier-Pinard, P., McDaid, H., and Horwitz, S. B. (2003) Mechanisms of Taxol resistance related to microtubules. *Oncogene 22*, 7280–7295.
14. ter Haar, E., Kowalski, R. J., Hamel, E., Lin, C. M., Longley, R. E., Gunasekera, S. P., Rosenkranz, H. S., and Day, B. W. (1996) Discodermolide, a cytotoxic marine agent that stabilizes microtubules more potently than Taxol. *Biochemistry 35*, 243–250.
15. Longley, R. E., Caddigan, D., Harmody, D., Gunasekera, M., and Gunasekera, S. P. (1991) Discodermolide—a new, marine-derived immunosuppressive compound. I. In vitro studies. *Transplantation 52*, 650–656.
16. Longley, R. E., Caddigan, D., Harmody, D., Gunasekera, M., and Gunasekera, S. P. (1991) Discodermolide—a new, marine-derived immunosuppressive compound. II. In vivo studies. *Transplantation 52*, 656–661.
17. Kowalski, R. J., Giannakakou, P., Gunasekera, S. P., Longley, R. E., Day, B. W., and Hamel, E. (1997) The microtubule-stabilizing agent discodermolide competitively inhibits the binding of paclitaxel (Taxol) to tubulin polymers, enhances tubulin nucleation reactions more potently than paclitaxel, and inhibits the growth of paclitaxel-resistant cells. *Mol. Pharmacol. 52*, 613–622.
18. He, L., Yang, C. P., and Horwitz, S. B. (2001) Mutations in beta-tubulin map to domains involved in regulation of microtubule stability in epothilone-resistant cell lines. *Mol. Cancer Ther. 1*, 3–10.
19. Klein, L. E., Freeze, B. S., Smith, A. B.III, and Horwitz, S. B. (2005) The microtubule stabilizing agent discodermolide is a potent inducer of accelerated cell senescence. *Cell Cycle 4*, 501–507.
20. Huang, G. S., Lopez-Barcons, L., Freeze, B. S., Smith, A. B., Goldberg, G. L., Horwitz, S. B., and McDaid, H. M. (2006) Potentiation of Taxol efficacy by discodermolide in ovarian carcinoma xenograft-bearing mice. *Clin. Cancer Res. 12*, 298–304.
21. Martello, L. A., McDaid, H. M., Regl, D. L., Yang, C.-P. H., Meng, D., Pettus, T. R. R., Kaufman, M. D., Arimoto, H., Danishefsky, S. J., Smith, A. B., and Horwitz, S. B. (2000) Taxol and discodermolide represent a synergistic drug combination in human carcinoma cell lines. *Clin. Cancer Res. 6*, 1978–1987.
22. Honore, S., Kamath, K., Braguer, D., Horwitz, S. B., Wilson, L., Briand, C., and Jordan, M. A. (2004) Synergistic suppression of microtubule dynamics by discodermolide and paclitaxel in non-small cell lung carcinoma cells. *Cancer Res. 64*, 4957–4964.

23. Martello, L. A., LaMarche, M. J., He, L., Beauchamp, T. J., Smith, A. B., and Horwitz, S. B. (2001) The relationship between Taxol and (+)-discodermolide: synthetic analogs and modeling studies. *Chem. Biol. 8*, 843–855.
24. Xia, S., Kenesky, C. S., Rucker, P. V., Smith, A. B.III, Orr, G. A., and Horwitz, S. B. (2006) A photoaffinity analogue of discodermolide specifically labels a peptide in beta-tubulin. *Biochemistry 45*, 11762–11775.
25. Canales, A., Matesanz, R., Gardner, N. M., Andreu, J. M., Paterson, I., Díaz, J. F., and Jiménez-Barbero, J. (2008) The bound conformation of microtubule-stabilizing agents: NMR insights into the bioactive 3D structure of discodermolide and dictyostatin. *Chem.—Eur. J. 14*, 7557–7569.
26. Murphy, D. B., and Wallis, K. T. (1983) Isolation of microtubule protein from chicken erythrocytes and determination of the critical concentration for tubulin polymerization in vitro and in vivo. *J. Biol. Chem. 258*, 8357–8364.
27. Smith, A. B.III, Kaufman, M. D., Beauchamp, T. J., LaMarche, M. J., and Arimoto, H. (1999) Gram-scale synthesis of (+)-discodermolide. *Org. Lett. 1*, 1823–1826.
28. Díaz, J. F., and Andreu, J. M. (1993) Assembly of purified GDP-tubulin into microtubules induced by taxol and taxotere: reversibility, ligand stoichiometry, and competition. *Biochemistry 32*, 2747–2755.
29. Parness, J., and Horwitz, S. B. (1981) Taxol binds to polymerized tubulin in vitro. *J. Cell Biol. 91*, 479–487.
30. Jain, A. N. (2007) Surflex-Dock 2.1: robust performance from ligand energetic modeling, ring flexibility, and knowledge-based search. *J. Comput.-Aided Mol. Des. 21*, 281–306.
31. Sobolev, V., Sorokine, A., Prilusky, J., Abola, E. E., and Edelman, M. (1999) Automated analysis of interatomic contacts in proteins. *Bioinformatics 15*, 327–332.
32. Rudiger, M., and Weber, K. (1993) Characterization of the post-translational modifications in tubulin from the marginal band of avian erythrocytes. *Eur. J. Biochem. 218*, 107–116.
33. Buey, R. M., Barasoain, I., Jackson, E., Meyer, A., Giannakakou, P., Paterson, I., Mooberry, S., Andreu, J. M., and Díaz, J. F. (2005) Microtubule interactions with chemically diverse stabilizing agents: thermodynamics of binding to the paclitaxel site predicts cytotoxicity. *Chem. Biol. 12*, 1269–1279.
34. Hyman, A. A., Salser, S., Drechsel, D. N., Unwin, N., and Mitchison, T. J. (1992) Role of GTP hydrolysis in microtubule dynamics: information from a slowly hydrolyzable analogue, GMPCPP. *Mol. Biol. Cell 3*, 1155–1167.
35. Nogales, E., Whittaker, M., Milligan, R. A., and Downing, K. H. (1999) High-resolution model of the microtubule. *Cell 96*, 79–88.
36. Li, H., DeRosier, D. J., Nicholson, W. V., Nogales, E., and Downing, K. H. (2002) Microtubule structure at 8 Å resolution. *Structure 10*, 1317–1328.
37. Mizuno, N., Toba, S., Edamatsu, M., Watai-Nishii, J., Hirokawa, N., Toyoshima, Y. Y., and Kikkawa, M. (2004) Dynein and kinesin share an overlapping microtubule-binding site. *EMBO J. 23*, 2459–2467.
38. Al-Bassam, J., Ozer, R. S., Safer, D., Halpain, S., and Milligan, R. A. (2002) MAP2 and tau bind longitudinally along the outer ridges of microtubule protofilaments. *J. Cell Biol. 157*, 1187–1196.
39. Huzil, J. T., Chik, J. K., Slysz, G. W., Freedman, H., Tuszynski, J., Taylor, R. E., Sackett, D. L., and Schriemer, D. C. (2008) A unique mode of microtubule stabilization induced by peloruside A. *J. Mol. Biol. 378*, 1016–1030.
40. Keskin, O., Durell, S. R., Bahar, I., Jernigan, R. L., and Covell, D. G. (2002) Relating molecular flexibility to function: a case study of tubulin. *Biophys. J. 83*, 663–680.
41. Anders, K. R., and Botstein, D. (2001) Dominant-lethal alpha-tubulin mutants defective in microtubule depolymerization in yeast. *Mol. Biol. Cell 12*, 3973–3986.
42. Kar, S., Florence, G. J., Paterson, I., and Amos, L. A. (2003) Discodermolide interferes with the binding of tau protein to microtubules. *FEBS Lett. 539*, 34–36.
43. Makrides, V., Massie, M. R., Feinstein, S. C., and Lew, J. (2004) Evidence for two distinct binding sites for tau on microtubules. *Proc. Natl. Acad. Sci. U.S.A. 101*, 6746–6751.
44. Freedman, H., Huzil, J. T., Luchko, T., Ludueña, R. F., and Tuszynski, J. A. (2009) Identification and characterization of an intermediate Taxol binding site within microtubule nanopores and a mechanism for tubulin isotype binding selectivity. *J Chem. Inf. Model. 49*, 424–436.
45. Smith, A. B.III, and Freeze, B. S. (2008) (+)-Discodermolide: total synthesis, construction of novel analogues, and biological evaluation. *Tetrahedron 64*, 261–298.
46. Hung, D. T., Nerenberg, J. B., and Schreiber, S. L. (1996) Syntheses of discodermolides useful for investigating microtubule binding and stabilization. *J. Am. Chem. Soc. 118*, 11054–11080.
47. Gunasekera, S. P., Longley, R. E., and Isbrucker, R. A. (2002) Semisynthetic analogues of the microtubule-stabilizing agent discodermolide: preparation and biological activity. *J. Nat. Prod. 65*, 1830–1837.